



Role of IR and UV-Vis Spectroscopies Combined with Electrical Measurements in Materials Relevant for Gas Sensing

Ambra Fioravanti¹(✉), Sara Morandi², Stefano Lettieri³, Michele Sacerdoti⁴, Pietro Marani¹, and Maria Cristina Carotta¹

¹ Istituto di Scienze e Tecnologie per l'Energia e la Mobilità Sostenibili (CNR-STEMS), 44124 Ferrara, Italy

ambra.fioravanti@stems.cnr.it

² Dipartimento di Chimica, Università di Torino, 10125 Torino, Italy

³ Istituto di Scienze Applicate e Sistemi Intelligenti "E. Caianiello" (CNR-ISASI), 80126 Napoli, Italy

⁴ Dipartimento di Fisica e Scienze della Terra, Università di Ferrara, 44122 Ferrara, Italy

Abstract. Wide band gap semiconductors are extensively used to realize sensors for the detection of a great variety of gases. The study of the sensing mechanism is at the base of the understanding, as well as the tuning, of the sensing properties. In this work, anatase and rutile, polymorphic forms of TiO₂ were considered to be characterized through a combined approach (based on spectroscopic techniques and electrical measurements) finalized to determine the processes involved in the detection mechanism during interaction with carbon monoxide.

Keywords: Thick film gas sensors · UV-Vis-NIR and FT-IR spectroscopies · Sensing mechanisms · Rutile · Anatase · TiO₂

1 Introduction

Today, gas sensors based on semiconducting metal oxides (such as SnO₂, ZnO, TiO₂, WO₃, etc.) are successfully used in many applications (for example in pollutant monitoring, in the control of industrial systems or food quality, in medical diagnosis, etc.) to detect a large number of gaseous compounds (CO, O₃, C₂H₄, NO_x, VOCs, etc.) [1]. They exploit the chemiresistive effect for which the interaction of a gas with their surface can induce a significant change in the electrical resistance/conductance of the oxide. Therefore, the electrical resistance/conductance is the main parameter typically recorded. It is a simple task but this does not provide direct information about the processes that occur during sensing. To describe the sensing mechanism of a specific material toward a specific gas, it is necessary to determine the electronic properties of the oxide during the interaction with the gas.

In this work, our proposed approach is based on the combination of the spectroscopic characterization of the oxide (absorbance FT-IR, diffuse reflectance UV-Vis-NIR) with

the electrical measurements performed on the related thick films. Indeed, the IR and UV-Vis spectroscopies represent a convenient experimental characterization to study the electronic properties and surface chemistry of metal oxides [2, 3]. When there are point defects in these oxides, there are shallow levels in the band gap, with an activation energy typically between 10^{-3} and 10^{-1} eV, being responsible for their semiconducting properties, thus for their gas sensing properties. It is possible to test these defect levels by the absorption of the electromagnetic radiation at specific energies and to detect the changes in level populations and in free carrier concentration by varying the temperature or the atmosphere.

Here, we focused our attention on the titanium oxide both in anatase and rutile phase as functional material. Anatase is a TiO_2 meta-stable phase which irreversibly transforms to rutile phase, that is thermodynamically stable, at temperatures higher than $600\text{ }^\circ\text{C}$ [4]. The pros and cons of using anatase or rutile in gas sensing have been debated since decades and discussion is still open [5]. In the following, the results of the combined approach (based on spectroscopic techniques and electrical measurements) to determine the processes involved in the detection mechanism for TiO_2 in anatase and rutile phase are reported in the case of carbon monoxide (CO) as interacting gas.

2 Materials and Methods

TiO₂ preparation – The anatase powder was synthesized via sol-gel route by dissolving Ti(IV) n-butoxide (Merck, 97%) in absolute ethanol to obtain a 0.23 M solution. Subsequently, an ethanol/water 1:1 vol. Solution was added drop by drop under rapid stirring to the first one. The mixture was filtered by gravity, washed with diethyl ether and dried at $90\text{ }^\circ\text{C}$ for 12 h in air, then calcined at $450\text{ }^\circ\text{C}$ for 2 h. To obtain the rutile sample, the anatase powder was annealed at $850\text{ }^\circ\text{C}$ for 1 h [6].

Morphological characterization – Powder morphology was studied with Field Emission Scanning Electron Microscopy (FE-SEM) by a Carl Zeiss Sigma microscope.

Structural analysis – X-ray diffraction (XRD) analyses were performed by using a Philips PW 1830 vertical diffractometer with Bragg–Brentano geometry. The unit cell parameters were estimated with FullProf software (structure profile refinement), while the crystallite size was calculated by Williamson-Hall method [7].

Spectroscopic characterization – Diffuse reflectance (DR) UV-Vis-NIR spectra were run at RT on a Varian Cary 5 spectrophotometer. For the analysis, the prepared powders were placed in a quartz cell, allowing thermal treatments in controlled atmosphere up to $800\text{ }^\circ\text{C}$. Spectra are reported with the Kubelka–Munk function [$f(R_\infty) = (1 - R_\infty)^2/2R_\infty$, where R_∞ is the reflectance of an ‘infinitely thick’ layer of the sample] in the ordinate scale [8]. Absorption FT-IR spectra were run on a Perkin-Elmer 2000 FT-IR spectrophotometer equipped with a Hg–Cd–Te cryodetector, working in the range of wavenumbers $7800\text{--}580\text{ cm}^{-1}$. The powders were compressed in self-supporting disks and placed in a commercial heatable stainless steel IR cell (Aabspec) allowing in situ thermal treatments up to $600\text{ }^\circ\text{C}$ and simultaneously spectra recording. For both UV-Vis-NIR and medium IR (MIR) analyses, samples were activated at $550\text{ }^\circ\text{C}$ in vacuum and in dry oxygen, then underwent treatment in CO at $400\text{ }^\circ\text{C}$.

Sensors fabrication – The thick films were deposited on miniaturized alumina substrates provided with Au contacts and heaters by screen printing and fired at 650 °C.

Electrical characterization – Sensors were tested by the flow-through technique with a constant flow rate of 0.5 L/min. Conductance vs. temperature was measured and the surface energy barrier obtained through temperature stimulated conductance measurement [9] both in dry air and in a mixture of dry air and CO. Sensor dynamic responses to CO in dry air were obtained at working temperatures between 350 and 550 °C.

3 Results and Discussion

SEM images showed a homogeneous size distribution of spherical particles both for anatase (Fig. 1A) and rutile (Fig. 1B) powders. As expected, a considerable grain growth occurs when the crystalline phase changes from anatase to rutile [10]. XRD patterns (Fig. 1C) confirm anatase (space group $I4_1/amd$) and rutile (space group $P4_2/mnm$) phases, providing a medium crystallite size of 12 and 101 nm, respectively.

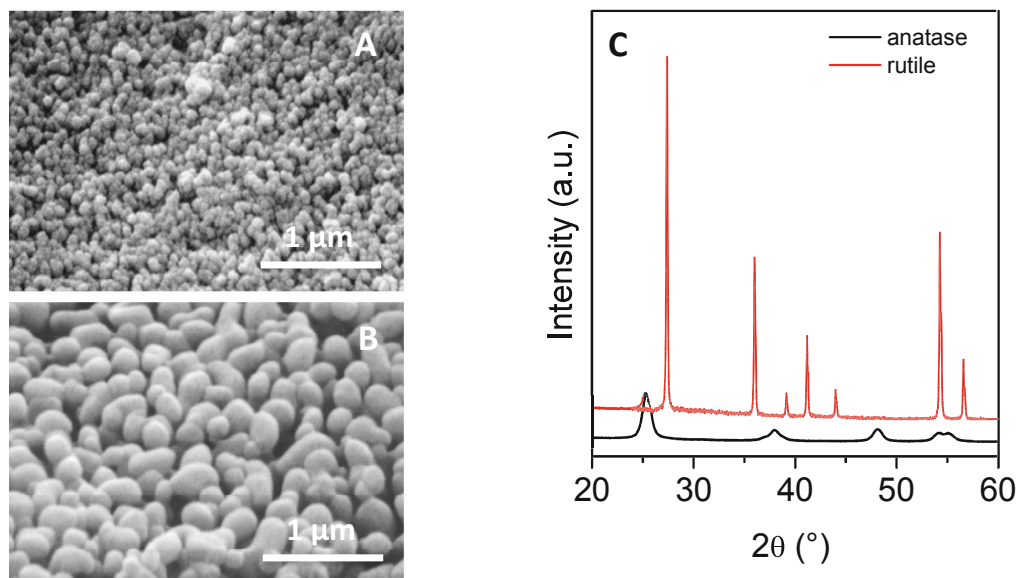


Fig. 1. SEM images of TiO₂ anatase (A) and rutile (B) powders and their XRD patterns (C).

The conductance vs. temperature curves (Arrhenius plots) in air (Fig. 2A) showed for both materials the n-type semiconductor behavior. The shape of the Arrhenius plots and the conductivity are very different for the two TiO₂ phases. At low temperature, anatase exhibits a conductivity about two orders of magnitude lower than the rutile one. On the other hand, the conductivity for the rutile film does not change in the temperature range 100–400 °C. The dry air/CO atmosphere induces an increase in the anatase conductance not observed for rutile sensor, implying better sensing performance for anatase sensor. This is confirmed, as it is shown in Fig. 3, where we report a comparison between the responses in dry air to 50 ppm of CO for TiO₂ anatase and rutile based sensor. Taking into account the surface energy barriers vs. temperature (Fig. 2B), we can observe higher barrier height in presence of reducing atmosphere, in particular for the anatase sensor.

This behavior appears immediately in disagreement with the sensing mechanism based on the Schottky barrier model for n-type semiconductors, already observed for example in ZnO and SnO₂ [11]. Such mechanism consists in a releasing of trapped electrons of ionosorbed oxygen atoms after a surface chemical reaction with a consequent decreasing of the barrier height and the increasing of conductance.

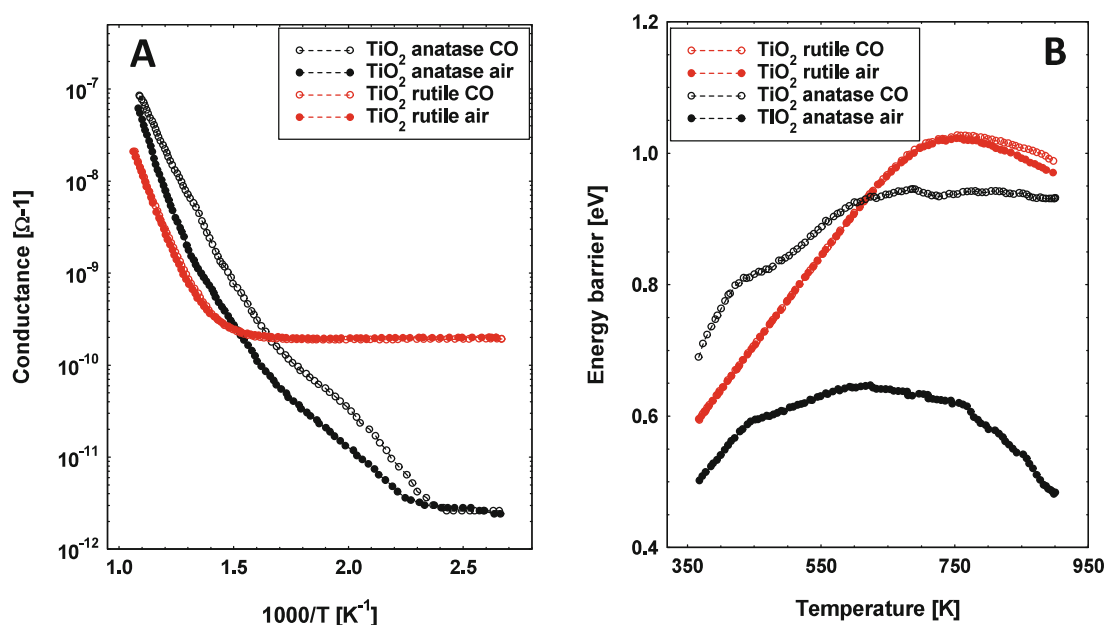


Fig. 2. For the two TiO₂ powders: comparison of conductance vs. temperature in dry air and in a mixture of dry air and CO (100 ppm) (A) and comparison of the energy barrier dependence on temperature in dry air and in a mixture of dry air and CO (100 ppm) (B).

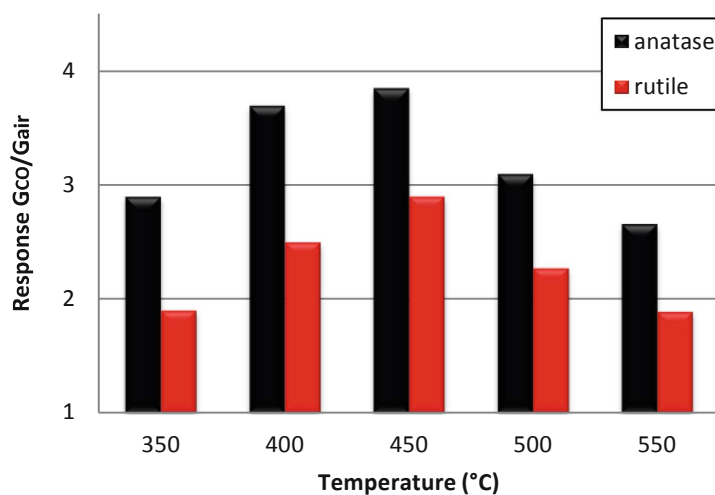


Fig. 3. Responses to 50 ppm of CO reported as G_{CO}/G_{air} obtained at different temperatures for the two TiO₂ powders.

The results of the spectroscopic characterization shed light to this unexpected behavior.

Figure 4 shows both the DR UV-Vis-NIR spectra (section A) and absorption spectra in the MIR region (section B) of anatase (black traces) and rutile (red traces). After

treatment in oxygen at 550 °C (dashed traces), the interaction with CO at 400 °C causes the formation of broad absorptions for both samples (solid traces).

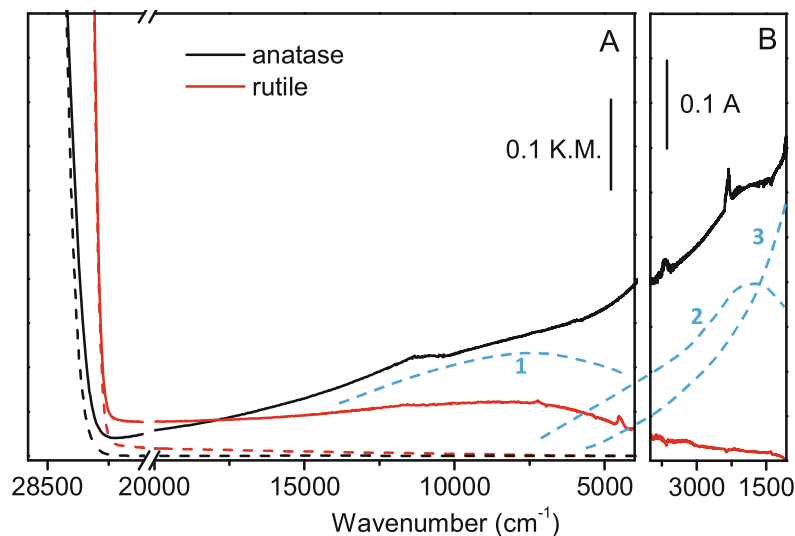


Fig. 4. Diffuse reflectance UV-Vis-NIR spectra (A) and absorption spectra in the MIR region (B) of anatase (black traces) and rutile (red traces) after treatment in oxygen at 550 °C (dotted traces) and after interaction with CO at 400 °C (solid traces).

It is well evident the different spectroscopic behavior of the two samples. In particular, for rutile the interaction with CO causes the formation of a broad band centered in the Vis-NIR spectral region with a weak tail in the medium IR region. This absorption is related to the presence of Ti^{3+} ions and assigned to a metal-metal charge transfer from Ti^{3+} to Ti^{4+} ions, also known as polaronic transition [12–14]. The absorption shown by anatase after interaction with CO at 400 °C is more complex. In this case, at least three contributions can be distinguished, as evidenced by dashed blue curves in the Fig. 4: 1) an absorption related to the polaronic transition already discussed for rutile; 2) an absorption centered in the MIR region and related to the photoionization of mono-ionized oxygen vacancies [15–17] and 3) an absorption that increases in intensity upon decreasing the wavenumbers, a feature characteristic of free electrons in the conduction band [18].

It is clear that an increase in conductance together with an increase in energy barrier height in CO atmosphere means that the electrons which enter the conduction band as a response to CO do not lower the barrier as foreseen by the Schottky barrier model. A similar behavior has been already seen for the mixed $Ti_xSn_{1-x}O_2$ oxides with $x \geq 0.3$, for which CO interacts with the surface lattice oxygen atoms whose bond electrons do not participate to the development of the spatial charge region and thus of the Schottky barrier [19]. Finally, it must be considered that the pure titania in rutile phase is affected by an exaggerated grain coalescence. In this case, the pinning of Fermi level can develop, so hindering the gas response; thereby it is reasonable that the two energy barriers, in air and in CO, do not differ significantly from one another, because very weak sensing process occurs [19].

References

1. Neri, G.: First fifty years of chemoresistive gas sensors. *Chemosensors* **3**, 1–20 (2015)
2. Dey, A.: Semiconductor metal oxide gas sensors: a review. *Mater. Sci. Eng. B Solid-State Mater. Adv. Technol.* **229**, 206–217 (2018)
3. ViterIgor, R., Barhoum, I.: Optical spectroscopy for characterization of metal oxide nanofibers. In: Barhoum, A., Bechelany, M., Makhlof, A. (eds.) *Handbook of Nanofibers*, pp. 523–556. Springer, Cham (2019). https://doi.org/10.1007/978-3-319-53655-2_10
4. Lettieri, S., Pavone, M., Fioravanti, A., Santamaria Amato, L., Maddalena, P.: Charge carrier processes and optical properties in TiO₂ and TiO₂-based heterojunction photocatalysts: a review. *Materials* **14**, 1645 (2021)
5. Zakrzewska, K., Radecka, M.: TiO₂-based nanomaterials for gas sensing—influence of anatase and rutile contributions. *Nanosc. Res. Lett.* **12**, 89 (2017)
6. Carotta, M.C., et al.: Comparison between titania thick films obtained through sol–gel and hydrothermal synthetic processes. *Thin Solid Films* **515**(23), 8339–8344 (2007)
7. Suryanarayana, C., Norton, M.G.: *X-Ray Diffraction: A Practical Approach*. Springer, New York (1998). ISBN 9781489901507
8. Kubelka, P.: New contributions to the optics of intensely light-scattering materials, part I. *J. Opt. Soc. Am.* **38**, 448–457 (1948)
9. Clifford, P.K., Tuma, D.T.: Characteristics of semiconductor gas sensors – II. Transient response to temperature change. *Sens. Actuat. B Chem.* **3**(83), 255–282 (1982)
10. Byrne, C., Fagan, R., Hinder, S., McCormack, D.E., Pillai, S.C.: New approach of modifying the anatase to rutile transition temperature in TiO₂ photocatalysts. *RSC Adv.* **6**, 95232–95238 (2016)
11. Fioravanti, A., Morandi, S., Carotta, M.C.: Spectroscopic–electrical combined analysis to assess the conduction mechanisms and the performances of metal oxide gas sensors. *Chemosensors* **10**, 447 (2022)
12. Cox, P.A.: *Transition Metal Oxides*. Clarendon Press Ed. (1992)
13. Mestl, G., Verbruggen, N.F.D., Knozinger, H.: Mechanically activated MoO₃. 2. Characterization of defect structures. *Langmuir* **11**, 3035 (1995)
14. Dieterle, M., Weinberg, G., Mestl, G.: Raman spectroscopy of molybdenum oxides part I. Structural characterization of oxygen defects in MoO_{3-x} by DR UV/VIS, Raman spectroscopy and X-ray diffraction. *PCCP* **4**, 812–821 (2002)
15. Özgür, Ü., et al.: A comprehensive review of ZnO materials and devices. *J. Appl. Phys.* **98**, 1–103 (2005)
16. Göpel, W., Lampe, U.: Influence of defects on the electronic structure of zinc oxide surfaces. *Phys. Rev. B: Condens. Matter Mater. Phys.* **22**, 6447–6462 (1980)
17. Carotta, M.C., et al.: (Ti, Sn)O₂ binary solid solutions for gas sensing: spectroscopic, optical and transport properties. *Sens. Actuat. B Chem.* **130**, 38–45 (2008)
18. Faglia, G., Baratto, C., Sberveglieri, G., Zha, M., Zappettini, A.: Adsorption effects of NO₂ at ppm level on visible photoluminescence response of SnO₂ nanobelts. *Appl. Phys. Lett.* **86**, 011923 (2005)
19. Carotta, M.C., et al.: (Ti, Sn) solid solutions as functional materials for gas sensing. *Sens. Actuat. B Chem.* **194**, 195–205 (2014)